JTTEE5 10:133-137

Plasma Spray Coating of Spray-Dried Cr_2O_3/wt.%TiO_2 Powder

B.K. Kim, D.W. Lee, and G.H. Ha

(Submitted 14 July 1999; in revised form 10 December 1999)

An agglomerated Cr_2O_3/wt.%TiO_2 powder has been fabricated by the spray drying process under different parameters. The spray-dried powder has well-agglomerated particles of spherical shape. In the conditions of the high slurry feed rate and low binder concentration in the slurry, the powder has large cavities inside some particles and ruggedness over their surface. The optimum plasma spray feed rate has been found by examining the spraying behavior of the powder and melted state of particles. The plasma spray coating has been performed under different process variables such as spraying distance and plasma power. These parameters strongly affect the characteristics of the coated layer: microstructure, hardness, and bond strength.

Keywords Cr_2O_3/TiO_2, feedstock, powder manufacture, spray dry

1. Introduction

Plasma spray coating with ceramic powders is widely used to improve the wear resistance and hardness of industrial parts.[1] Properties of plasma-sprayed coatings are affected by their microstructure, which depends critically on the characteristics of powders and plasma spray conditions such as the spray distance, plasma power, and powder feed rate. High flowability of a powder is a prime requirement for a good plasma spray process. A high apparent feedstock density can result in a dense coated layer with a lamella structure resulting from energetic particle impact against the substrate and effective particle flatting.

The ceramic powders applied by plasma spray can be produced by two processes.[2] One is spray drying in which the powders are agglomerated from fine raw powders.[3] The agglomerated spray-dried powders have a low apparent density due to the formation of many pores inside the agglomerates, which consist of a great number of fine particles. This method achieves more uniform sized powders of spherical shape and also enables the production of composite powders.[4] Other process methods such as fusing and crushing produce particles of irregular shape.

In this study, a spray-dried mixture of Cr_2O_3/3wt.%TiO_2 powders was used. The spray drying process was performed under various conditions to maximize the apparent density and flowability of the powder mixture. The powders were sprayed under various process parameters and the coated layers were examined with respect to their microstructure, hardness, and bond strength.

B.K. Kim, **D.W. Lee**, and **G.H. Ha** Materials Science Department, Korea Institute of Machinery & Materials, 66 Sangnam-Dong Changwon, Kyungnam, Korea.

2. Experimental Procedure

The slurry for spray drying was made of distilled water, raw Cr_2O_3 (~1 μm) and TiO_2 (~1 μm) powders, and PVA (polyvinyl-alcohol). The spray drying was performed in a centrifugal atomizer-type spray dryer (model DJE003R, Dongjingiyun Ltd., Inchun, Korea) with a disk diameter of 66 mm, rotation speed of 11,000 rpm, and chamber temperature of 110 °C. The main process parameters of spray drying were varied inside ranges of 11 to 23 wt.% for the powder concentration in the slurry, 0.5 to 3.0 wt.% for the PVA concentration with respect to the powder, and 28 to 180 g/min in the slurry feed rate. The morphology and cross-sectional microstructure of the spray-dried powder were observed with a scanning electron microscope (SEM), and the flowability and apparent density were measured by the standard method of ASTM B 213-83 and 214-86.

The powders were sieved below 75 μm and then sprayed into water with a plasma torch (model Metco 9MB, Sulzer Metco Ltd., Hialeah, FL) at a feed rate varying from 30 to 95 g/min to find the optimum feed rate, that provides good uniform flowability and melted state of particles. The other spray parameters were fixed to a plasma power of 35 kW and the reaction gas pressures of 100 psi in argon and 25 psi in hydrogen. The coatings were deposited on aluminum substrates of 20 mm diameter at spray distances from 6 to 11 cm and plasma power from 39 to 51 kW. The cross-sectional microstructure of coated layers was observed by SEM and the average hardness were measured from ten random indentions. The bond strength between the substrate and coated layer was measured in tension test after attaching cylindrical jigs on both sides of coating samples (ASTM C-633).

3. Results and Discussion

3.1 Effect of Spray Drying Condition on Powder Properties

The agglomerated powders were formed through three steps of spray drying: (1) transfer of the slurry to the rotating disk, (2)

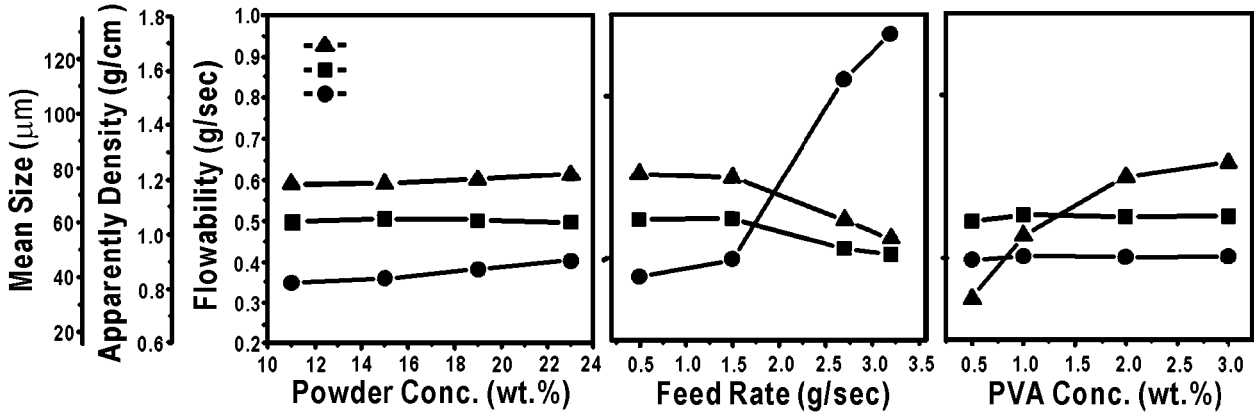

Fig. 1 Characteristics of powders produced with different spray drying conditions

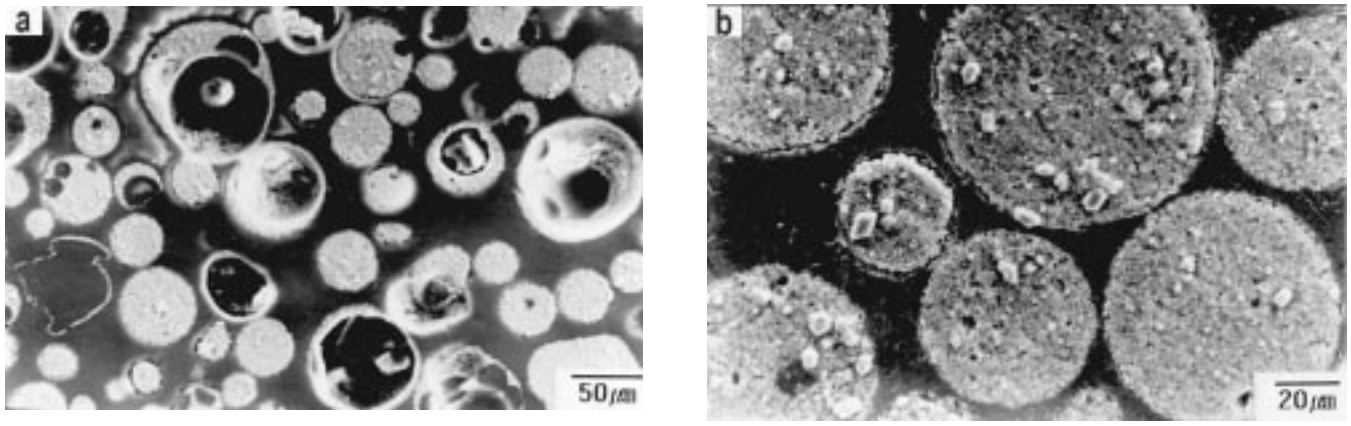

Fig. 2 Cross-sectional SEM microstructures of (**a**) hollowed and (**b**) well-agglomerated spray-dried powders

atomization of the slurry into droplets by the centrifugal force on the rotating disk, and (3) formation of spherical aggregates from moisture evaporation in the hot chamber.[5]

Characteristics of the spray-dried powders are mainly affected by the size and physical properties of the atomized slurry droplets. Figure 1 shows the dependence of the mean size, apparent density, and flowability of the powders produced under the different spray drying parameters. The mean size of spray-dried powder particles slightly increases from 37 to 45 μm with increasing powder and binder concentrations in the slurry and indicates that an increase of slurry viscosity causes a growth in droplet size.[6] On the other hand, coarse powders with the average particle size of ~120 μm were formed at the high slurry feed rate of about 160 g/min.

The atomized droplets experience two effects in the hot chamber. One is the evaporation of moisture, the other is agglomeration of particles due to this evaporation. The high slurry feed rate ensures that large droplets are formed during atomization. As a result, water is not fully evaporated but transferred locally to only the surface region. Then inner moisture moves to the aggregate surface and transports the inner powder particles by capillary force, thereby creating large hollow regions inside dried powder aggregates (Fig. 2 (a)). Therefore, the apparent density of powder produced with the feed rate near 160 g/min is considerably less in comparison to powders manufactured at a lower rate. The hollow aggregates are very light and can be easily broken into small particles.

Variation of the binder concentration does not change the size and apparent density of the powders. The flowability increases with increasing binder content until the maximum value of 0.6 g/cc at about 2 wt.% of the PVA concentration is reached. Even if the powder density and particle size remain almost the same, the flowability of the powder can decrease due to surface roughness, which forms due to poor adhesion between the raw powder particles.

The slurry feed rate of 85 g/min, powder concentration of 19 wt.%, and PVA concentration of 2 wt.% were selected as optimum spray drying conditions, which maximized the flowability and apparent density of the powder (Fig. 2 (b)). As a result, powder particles of spherical shape, which were 25 to 60 μm in size, were well agglomerated without any inner cavities.

Powders passed through a plasma flame at a feed rate from 30 to 70 g/min and, when cooled under water, appeared green and dark gray in color. A powder produced with the feed rate of about 90 g/min exhibited only a dark gray color, which indicated a well-melted state (Fig. 3). The increase of the feed rate up to around 90 g/min improved the flow behavior and melted state of the powder and increased its average density from 2.14 to 2.25 (±0.01) g/cc.

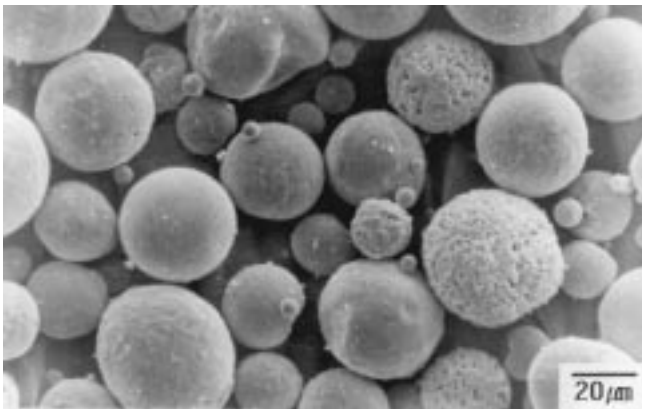

Fig. 3 SEM morphology of plasma-treated powders produced with the feed rate of 90 g/min

3.2 Effect of plasma spray condition on properties of coated layer

The plasma spray coating can be densely deposited if optimum plasma spray conditions are used. The density of the coated layer is affected by the powder feed rate, spray distance, and plasma power, since these change the velocity and melted state of the particles moving in the plasma gun.

The cross-sectional microstructures of plasma-sprayed coatings processed under different spray distances are shown in Fig. 4. The coatings formed at spray distances of 6 or 11 cm exhibit some porosity, while that obtained at 9 cm exhibits a relatively dense structure.

The velocity of the particles can be increased within a short time by the high velocity of the plasma jet, and then continuously decreased with the aim of determining a critical distance that provides an optimal velocity and an impact force on particles during coating formation. The temperature of the particles can also be changed in a similar fashion.

At a spray distance of 6 cm, although the particle velocity is probably not much different than at 9 cm, the particles can be easily splashed or fragmented into the precursor powders during collision, since the heat transfer is insufficient to fuse all the particles. This will result in the formation of pores in the coating, leaving unmelted aggregates.

In the case of a spray distance of 11 cm, although enough melting of agglomerates can occur, the particle velocity may significantly drop and cause formation of high porosity because of low impact energy. As shown in Fig. 5, when the spray distance is as long as 9 cm, this speculation corresponds well with the maximum hardness (1080 Hv) and bond strength (21.8 MPa). This arises due to an increase in the fraction of the real contact area between the coated layer and substrate owing to the effective deformability of the partially melted particles and their high impact. The maximum hardness and bond strength of the layer coated with spray-dried powder are compared with that of the layer coated by commercial fused/crushed power (1095 Hv, 16.8 MPa). The maximum hardness value is similar, but the bond strength is improved.

Thus, using the critical spray distance, the particles can be effectively flattened to thin disks, which result in the maximum hardness and bond strength. These results and microstructures

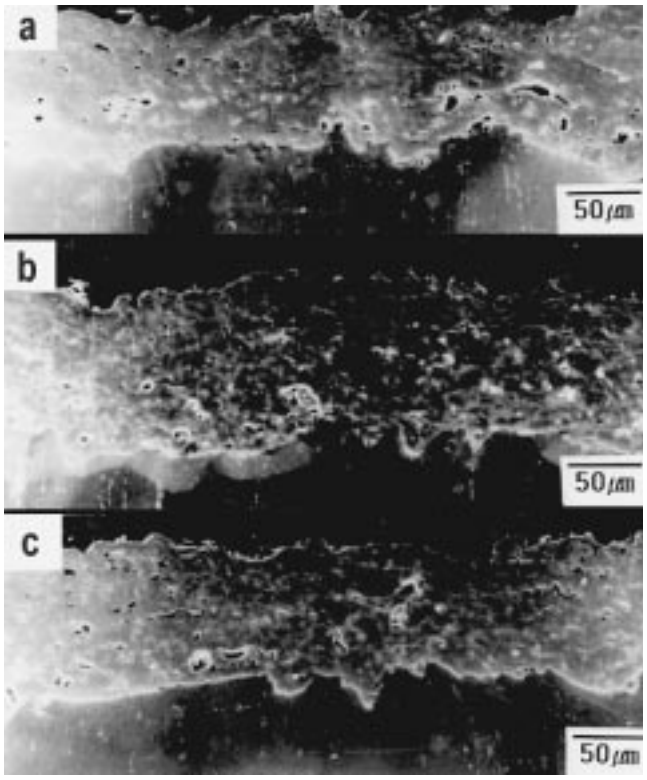

Fig. 4 Cross-sectional microstructures of plasma spray layers coated with the plasma power of 43 kW and the spraying distance of (**a**) 6 cm, (**b**) 9 cm, and (**c**) 11 cm

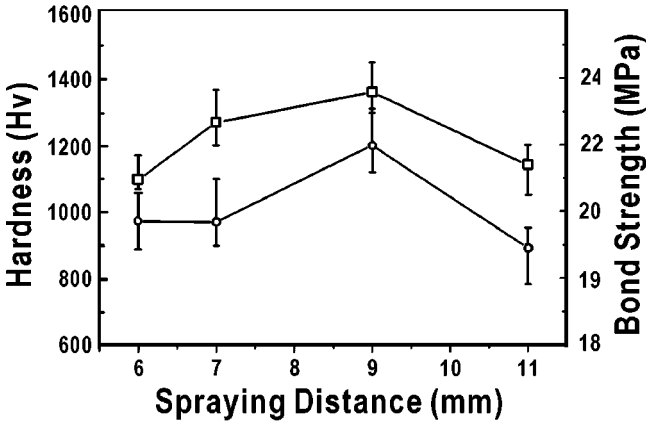

Fig. 5 Effect of the spraying distance on hardness and bond strength of plasma spray layers coated with the plasma power of 43 kW

shown in Fig. 4 indicate that the critical spray distance for the powder is 9 cm and this provides the most dense coating.

The cross-sectional microstructures of coated layers obtained at different power levels and a fixed spray distance of 9 cm are shown in Fig. 6. The layer deposited at 39 kW exhibits more pores because of the presence of unmelted particles. The coating produced at 47 kW is relatively dense; however, a coating formed at 51 kW (Fig. 6c) exhibits the

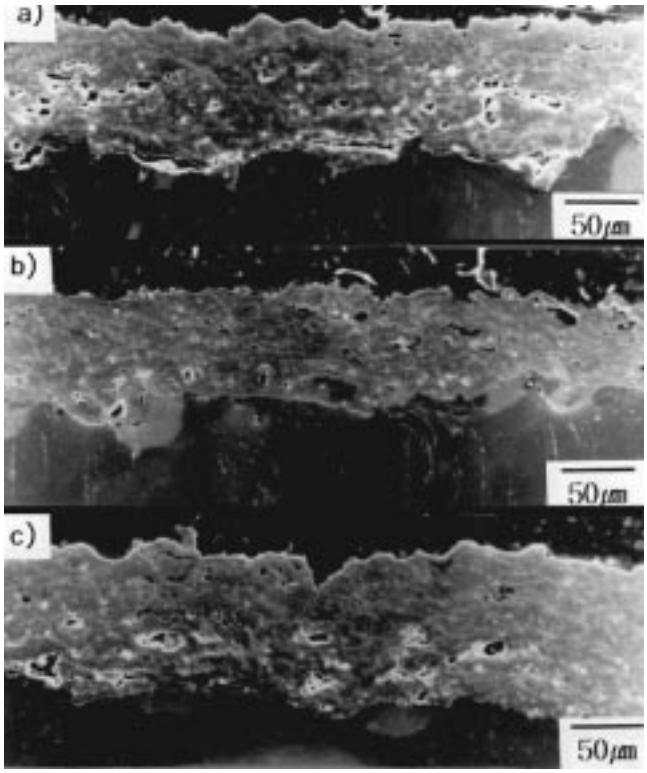

Fig. 6 Cross-sectional microstructures of plasma spray layers coated with the spraying distance of 9 cm and plasma power of (**a**) 39 kW, (**b**) 47 kW, and (**c**) 51 kW

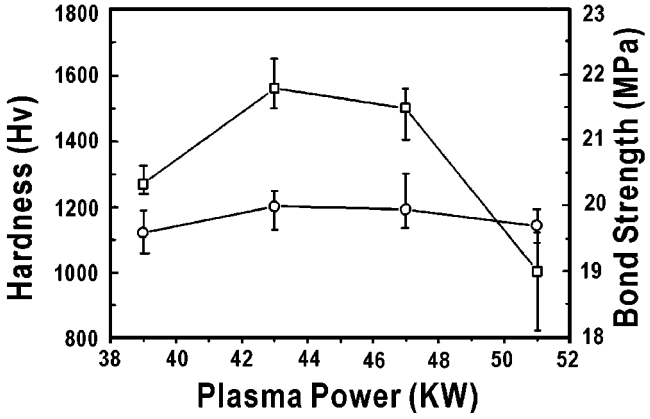

Fig. 7 Effect of the plasma power on hardness and bond strength of plasma spray coated layers

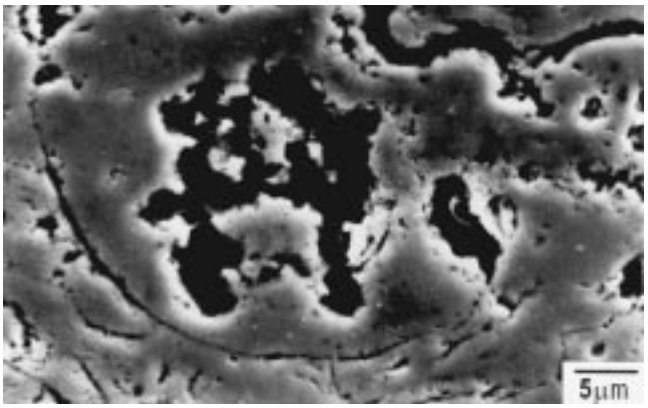

Fig. 8 Cross-sectional SEM microstructure of a plasma spray coated layer with the inner voids within deposited particles

some amount of large voids as the coating formed under the low power condition.

The droplets must be flattened into thin disks and solidified without any splashing to minimize porosity in a coating. The high plasma energy increases the temperature and velocity of the spray-dried powder aggregates and may break up or splash splats.[7] Thus, the high porosity of the coated layers obtained at 51 kW may result from poor flow behavior and poor deposition efficiency of the powder.

Dependencies of the micro-Vickers hardness and bond strength of the coated layer on the plasma power are presented in Fig. 7. The hardness of the coating deposited under a plasma power outside the range of around 43 to 47 kW does not change significantly. At 40 kW, the low bond strength may result from a decrease of the fraction of the real contact area, due to the presence of unmelted powder particles at the interface. The bond strength of coatings deposited at 51 kW is also slightly reduced. This decrease is caused by two reasons. One is the existence of large residual stresses at the interface formed as a result of interaction of compression stresses in the metal substrate and tensile stresses in the coating.[8] The other is the decrease in the fraction of the real contact area at the interface owing to splashing the splats.

The magnified images of dense areas inside coatings represented in Fig. 4(b) and 6(b) show that the inner voids are not of flattened powders (Fig. 8). This morphology arises due to the effect of binder evaporation. Therefore, to minimize coating porosity, the spray-dried powder must be produced with characteristics of high density and small particle size.

4. Conclusions

A spray-dried Cr_2O_3/3wt.% TiO_2 powder for plasma spray coating has been produced with optimal powder characteristics. The powder manufactured at high powder concentrations, high feed rates, and the lack of the binder in the slurry was not suitable for plasma spraying because of its low apparent density and flowability. These characteristics resulted from the formation of large cavities inside particles and their high local surface roughness.

The spherical powder particles produced for thermal spray coating were around 45 μm in size. The coated layer had the best properties if it was produced under the plasma spray conditions of spray distance 9 cm, power 47 kW, and feed rate 90 g/min, which provide the agglomerated particles with a high velocity and an appropriate melted state.

Acknowledgment

The authors are indebted to Professor A. P. Savitskii, Institute of Strength Physics and Materials Science (Tomsk, Russia) for helpful discussion and remarks.

References

1. C.P. Howes: *Fabricator*, 1995, vol. 20 (5), pp. 48-49.
2. S.Y. Hwang, B.G. Seoung, and M.C. Kim: *J. Kor. Powder Metall. Inst.*, 1996, vol. 3 (2), pp. 79-85.
3. D.W. Lee, G.G. Lee, B.K. Kim, and G.H. Ha: *J. Kor. Powder Metall. Inst.*, 1997, vol. 5 (1), pp. 28-34.
4. E. Lugscheider, M. Loch, and H.G. Suk: *Proc. Int. Thermal Spray Conf. Exp.*, 1992, pp. 555-59.
5. S.J. Lukasiewics: *J. Am. Ceram. Soc.*, 1989, vol. 72 (4), pp. 617-24.
6. K. Masters, and M.F. Mohtadi: *Br. Chem. Eng.*, 1967, vol. 12 (12), pp. 1890-92.
7. C.J. Li, J.L. Li, W.B. Wang, and K. Tani: *Thermal Spray: Meeting the Challenges of the 21st Century*, C. Coddet, ed., ASM International, Materials Park, OH, 1998, pp. 481-87.
8. S. Tobe: *J. Jpn. Thermal Spraying Soc.*, 1998, vol. 35 (1), pp. 65-73.